

**Dynamics of side-chain liquid-crystalline polymers: A dielectric spectroscopy investigation**M. Mierzwa,<sup>1</sup> G. Floudas,<sup>1,\*</sup> and A. Wewerka<sup>2</sup><sup>1</sup>*Foundation for Research and Technology–Hellas (FORTH), Institute of Electronic Structure and Laser, P.O. Box 1527, 711 10 Heraklion, Crete, Greece*<sup>2</sup>*Technical University Graz, Institute of Chemical Technology of Organic Substances (ICTOS), 8010 Graz, Austria*

(Received 28 February 2001; published 14 August 2001)

We have studied the dynamics in two side-chain liquid-crystalline derivatives of poly(norbornene diethyl-ester) with dielectric spectroscopy within the temperature range 190–433 K and the pressure range 1–3000 bars. Optical microscopy, x-ray scattering, and differential scanning calorimetry (DSC) revealed the formation of a nematic- and a smectic-A phase, respectively, in the polymers with the shorter and longer spacers. Multiple relaxation processes exist originating from the backbone and mesogenic dipoles. In the smectic-A phase two relaxation processes exist above the DSC glass temperature ( $\alpha$  and  $\alpha'$ ) which merge with decreasing temperature or with increasing pressure, thus suggesting a common molecular mechanism. The faster process is the segmental ( $\alpha$ ) relaxation associated with the dynamic glass transition, whereas the slower process reflects mainly the side-chain dynamics within the smectic layers. Pressure was found to increase the glass temperature in the nematic and smectic phases and the  $dT_g/dP$  was 18.7 and 16.9 K/kbar, respectively. However, the effect of pressure in inducing the isotropic-to-smectic transition is more drastic as  $dT_{SI}/dP = 26.4$  K/kbar.

DOI: 10.1103/PhysRevE.64.031703

PACS number(s): 64.70.Md, 61.41.+e, 77.84.Nh

**I. INTRODUCTION**

In the past 20 years, there has been a major interest in the synthesis of side-chain polymer liquid crystals (SC-PLC) where the mesogenic unit is located on the side chain of the polymer backbone [1–3]. These polymers have many commercial applications, such as high-strength materials for use in optical and electro-optical devices. In many of these applications, it is the reorientational dynamics of the mesogen and of the backbone that determines the response of the system in an external field.

In a series of investigations [4–13], mainly on oriented samples, the single relaxation in the isotropic phase was found to split into two processes by entering the nematic phase, which could be separately observed by choosing different orientations of the director. The slower relaxation (called the  $\delta$  process) was attributed to the end-to-end reorientation of the longitudinal dipole moment in the mesogenic group about its short molecular axis. Since it is this component that carries most of the dipole moment, the slower process was found to be the most intense. In the smectic-A phase, this mode was interpreted as being due to the side group flipping around the polymer backbone as the mesogen was hopping from one smectic layer to another. The faster relaxation (called the  $\alpha$  process), was attributed to transverse dipole moments rotating about the mesogens long axis. However, steric hindrance prevents a simple reorientation of the side-chain mesogen about its long or short axes giving rise to highly cooperative processes involving both rotation and translation of the mesogen and of its immediate environment. The evidence for cooperativity comes from a strong temperature dependence of the relaxation times and spectral broadening.

The theory of aligned nematic SC-PLC was developed by Attard and co-workers [14,15] as an extension of the Maier, Martin, and Saupe theory [16] of low molecular mass liquid crystals. According to the theory, the splitting of the relaxation in the nematic phase is due to the nematic potential which leads to the retardation of the slower process and the concomitant acceleration of the faster process, the magnitude of the effect depending on the nematic order parameter. Subsequent experiments investigated the effect of spacer length [5,7] and of surface treatment [9,13] on the relaxation processes of SC-PLC. It was found that increasing the spacer length further splits the two relaxations, whereas surface treatment can induce macroscopic alignment and affect the spectral shape.

Although the effect of temperature in inducing the phase transitions in SC-PLC has been studied extensively, there is only one report [17] where pressure was employed to study the dynamics and the thermodynamic changes associated with it. Pressure has been very successful in the past in the separation of mixed relaxation processes, like the segmental ( $\alpha$ ) from the more local  $\beta$  process [18,19]. More recently [20,21], we have studied the effect of pressure on a longer length scale, i.e., of the size of the end-to-end vector. We found that pressure exerts a stronger influence on the segmental ( $\alpha$ ) as compared to the global chain dynamics. Pressure was also employed in systems of current interest where the thermodynamics play a role. For example, it was found to induce dynamic miscibility in an athermal diblock copolymer [22]. Lastly, recent experimental efforts [23,24] have treated the effect of pressure on the crystallization process with emphasis on the *in situ* monitoring of the crystallization process.

In the present investigation we employ pressure in addition to temperature to study the complex dynamics in two SC-PLC derivatives of poly(norbornene diethyl-ester) with different spacer lengths giving rise to nematic and smectic-A mesophases. Since pressure leads to the densification of the material, it strongly affects the dynamics, mainly by slowing down the relaxation processes. However, different processes

\*Corresponding author. Present address: Department of Physics, University of Ioannina, 45110 Ioannina, Greece.

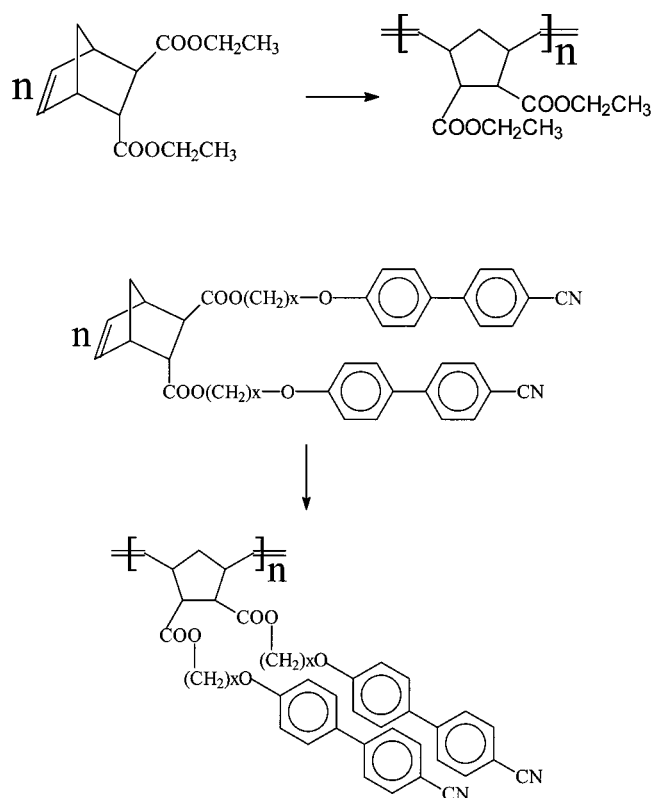


FIG. 1. Synthesis and structure of the poly(norbornene-diethylester) and the LC homopolymers.

have different volume requirements and thus pressure can be helpful in their identification. The two relaxation processes in the smectic-*A* phase are shown to have a common origin. The effect of pressure on inducing the isotropic-to-smectic transition is stronger than the shift of the glass transition temperature. The present work demonstrates that the dynamic state of such complex materials can only be completely accounted for if both temperature and pressure are specified.

## II. EXPERIMENT

Liquid-crystalline (LC) monomers based on a norbornene dicarboxylic acid were synthesized [25,26], bearing 4'-cyanobiphenyl groups as mesogenic units, which were coupled to the core unit via alkylene spacers with three or nine methylene groups. The length of the spacer is responsible for the formation of a nematic or a smectic mesophase (see below) in the SC-PLC with  $x=3$  (indicated as *H3*) and  $x=9$  (indicated as *H9*), respectively. The backbone polymer poly(norbornene diethylester) (more exact poly(diethylbicyclo[2.2.1]-hept-5-enedicarboxylate)) was also used in the present investigation (see Fig. 1).

The homopolymer polymerization reactions were carried out under inert conditions in a glove box via ROMP (ring opening metathesis polymerization) employing a Schrock-type molybdenum alkylidene initiator in absolute chlorobenzene. Due to the living character of the ROMP, this methodology provided well defined polymers with exact molecular weight and low polydispersity. Therefore this polymerization

reaction is a useful tool to get well defined block copolymers. The molecular weights were determined by gel permeation chromatography (GPC) with THF as solvent using the following arrangement: a Merck Hitachi L6000 pump, separation columns of Polymer Standards Service,  $8 \times 300$  m STV  $5 \mu\text{m}$  grade size ( $10^6$ ,  $10^4$ , and  $500 \text{ \AA}$ ); a refractive index detector from Wyatt Technology, and a model Optilab DSP interferometric refractometer; polystyrene standards obtained from Polymer Standards Services were used for calibration.

A Zeiss Axioskop 2 polarizing optical microscope was used together with a Linkam heating stage (THMS 600) and a TP93 temperature programmer (heating and cooling rates of 0.1 to 90 K/min). The system is also capable of monitoring the kinetics in real time by continuous recording using a charge-coupled device (CCD) camera ( $\frac{1}{2}$ " SONY color camera) and a fast frame grabber (capable of up to 50 frames/s). The experiments were made by heating to an initial temperature corresponding to the isotropic state followed by subsequent cooling to temperatures corresponding to the liquid-crystalline structures. Subsequently images were taken while heating the samples over the smectic-isotropic and nematic-isotropic transition temperatures. Representative optical microscopy images for the SC-PLC *H9* and *H3* are shown in Fig. 2 with macroscopic textures reminiscent of a smectic *A* and a nematic mesophase, respectively. The two images shown for *H9* and *H3* polymers were taken at 393 and 360 K with the same magnification.

A Polymer Laboratories DSC capable of programmed cyclic temperature runs over the range 113–673 K was used. Samples were first heated with a rate 10 K/min to temperatures corresponding to the isotropic state and subsequently cooled to 153 K with the same rate. The experiment was repeated with several different rates and the results for the transition temperatures and enthalpies obtained with the lowest rates (4 K/min) are shown in Table I. Typical DSC traces are shown in Fig. 2 on cooling and subsequent heating and indicate an exothermic peak on cooling due to the formation of the LC mesophase followed by an endothermic peak on heating signifying the dissolution process.

The setup for the pressure-dependent dielectric measurements consisted of the following parts: temperature-controlled sample cell, hydraulic closing press with pump and pump for hydrostatic test pressure. Silicon oil was used as the pressure transducing medium. The sample cell consisted of two electrodes with 20 mm in diameter and the sample with a thickness of  $50 \mu\text{m}$ . The sample capacitor was sealed and placed inside a Teflon ring to separate the sample from the silicon oil. The dielectric measurements were made at different temperatures in the range 253–363 K for pressures in the range from 1 bar to 3 kbars, and for frequencies in the range from  $10^{-2}$  to  $10^6$  Hz using a Novocontrol BDS system composed from a frequency response analyzer (Solartron Schlumberger FRA 1260) and a broadband dielectric converter. The complex dielectric permittivity  $\epsilon^* = \epsilon' - i\epsilon''$ , where  $\epsilon'$  is the real and  $\epsilon''$  is the imaginary part, is a function of frequency  $\omega$ , temperature  $T$ , and pressure  $P$ ,  $\epsilon^* = \epsilon^*(\omega, T, P)$ . For the *H9* phase additional measurements at higher frequencies were made ( $10^6$ – $10^9$  Hz). In

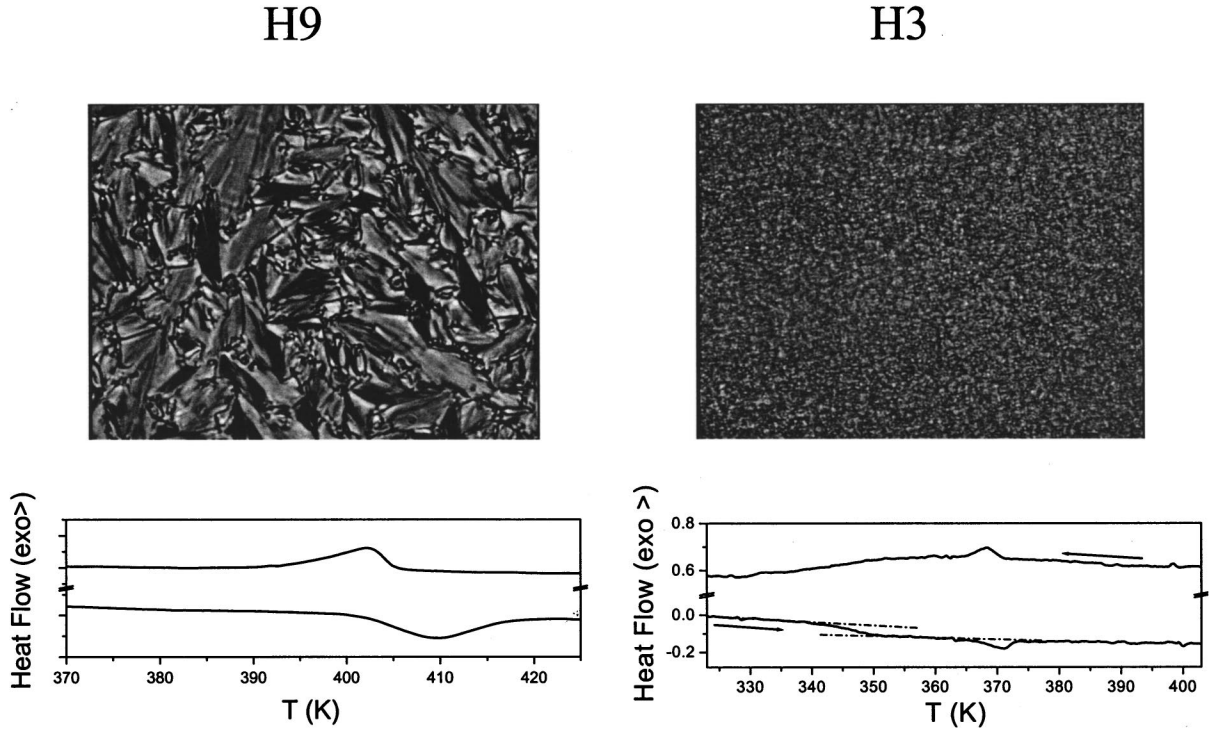


FIG. 2. Optical micrographs of the homopolymer *H9* (left) and *H3* (right) thin films observed between crossed polarizers at 393 and 360 K, respectively. The structures correspond to smectic-A (*H9*) and nematic (*H3*) phases. The DSC traces of the two samples are also shown on cooling and subsequent heating (rate of 4 K/min).

Figs. 3 and 4, representative dielectric permittivity and loss spectra are shown under isobaric ( $P=1$  bar) conditions for the SC-PLC *H3* and *H9*, respectively. In Fig. 3 the spectra are representative of all relaxations in the *H3* polymer, whereas for the *H9* polymer only spectra at higher temperatures are shown, for clarity. The spectra for the *H3* polymer (in Fig. 4, only the high-temperature processes are shown) reveal multiple relaxation processes which are indicated with the Greek letters  $\delta$ ,  $\gamma$ ,  $\beta$ , and  $\alpha$  by increasing temperature (we have used the traditional nomenclature for polymeric relaxation processes). It is the latter ( $\alpha$ ), however, that carries most of the intensity and has the steeper  $T$  dependence of the loss maximum (see below). Four processes were also found in the *H9* polymer, two above and two below the differential scanning calorimetry (DSC) glass transition  $T_g$  (indicated as  $\delta, \gamma$  and  $\alpha, \alpha'$ , respectively). The high-temperature spectra of *H9* display two main processes which are better depicted in the permittivity than the loss spectra due to the strong conductivity contribution in the latter. In the analysis of these high- $T$  spectra we have used a method [27] based on the derivative of the dielectric permittivity which has proven

successful. The derivative method yields  $\varepsilon'' \approx -(\pi/2) \times [\partial \varepsilon'(\omega)/\partial \ln \omega]$  as a conduction-free dielectric loss peak and the result is shown in the inset to Fig. 4, where the “fast” and “slow” processes are depicted as  $\alpha$  and  $\alpha'$ , respectively. In the analysis of the remaining dielectric spectroscopy (DS) spectra we have used the empirical equation of Havriliak and Negami (HN) [28],

$$\frac{\varepsilon^*(T, P, \omega) - \varepsilon_\infty(T, P)}{\Delta \varepsilon(T, P)} = \frac{1}{\{1 + [i\omega\tau_{\text{HN}}(T, P)]^\alpha\}^\gamma}, \quad (1)$$

where  $\tau_{\text{HN}}(T, P)$  is the characteristic relaxation time in this equation,  $\Delta \varepsilon(T, P) = \varepsilon_o(T, P) - \varepsilon_\infty(T, P)$ , is the relaxation strength of the process under investigation and  $\alpha, \gamma$  describe, respectively, the symmetrical and asymmetrical broadening of the distribution of relaxation times. In the fitting procedure we have used the  $\varepsilon''$  values at every temperature and pressure and in some cases the  $\varepsilon'$  data were also used as a consistency check. The linear rise of the  $\varepsilon''$  at lower frequencies is caused by the conductivity [ $\varepsilon'' \sim (\sigma_0/\varepsilon_0)\omega^{-1}$ , where  $\sigma_0$  is the dc conductivity and  $\varepsilon_0$  is the permittivity of free space] and has been included in the fitting procedure.

TABLE I. Molecular characteristics and transition temperatures of the two homopolymers.

Sample	$M_w$	$M_z$	PDI	$T_g$ (K)	$T_{\text{transition}}$ (K)	$\Delta H$ (J/g)
<i>H3</i>	35 200	48 200	1.44	344	$\overset{383}{N \rightarrow I}$	0.6
<i>H9</i>	27 000	45 500	1.58	294	$\overset{408}{S \rightarrow I}$	5

### III. RESULTS AND DISCUSSION

Four dielectrically active relaxation processes ( $\delta, \beta, \gamma, \alpha$ ) exist in the *H3* polymer and the relaxation times corresponding to the maximum loss for each process are plotted in Fig. 5, in the usual Arrhenius representation. Three of these processes display a linear dependence in this representation

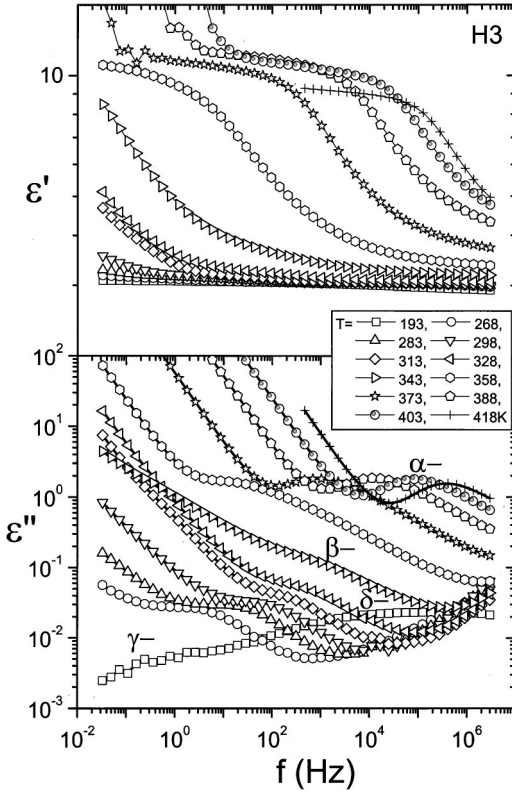


FIG. 3. Dielectric permittivity and loss spectra of the SC-PLC *H3* at some selected temperatures as indicated. Four processes are shown by the Greek letters  $\alpha, \beta, \gamma, \delta$  in the dielectric loss spectra.

whereas the one at higher temperatures ( $\alpha$ ) is curved. The  $\tau(T)$  dependence for the  $\delta$ ,  $\gamma$ , and  $\beta$  relaxations can be described by the Arrhenius dependence

$$\log_{10} \tau = \log_{10} \tau_0 + \frac{E}{2.303RT}, \quad (2)$$

where  $\tau_0$  is the high-temperature intercept and  $E$  is the activation energy. Alternatively, the  $\tau(T)$  dependence of the  $\alpha$  relaxation can be described by the well-known Vogel-Fulcher-Tammann (VFT) equation,

$$\log_{10} \tau = \log_{10} \tau_0 + \frac{B}{T - T_0}, \quad (3)$$

where  $B$  is the apparent activation energy and  $T_0$  is the “ideal” glass transition temperature. In the *H9* polymer, four dielectrically active processes exist ( $\delta, \gamma, \alpha, \alpha'$ ), two below ( $\delta, \gamma$ ) and two above ( $\alpha, \alpha'$ ) the DSC glass transition, and the corresponding characteristic relaxation times are plotted in Fig. 6. The two processes below  $T_g$  display a linear dependence and Eq. (2) was employed, whereas for the two processes above  $T_g$ , the VFT equation was employed. The parameters extracted from the fits of the  $\tau(T)$  for all processes are summarized in Tables II and III for the *H3* and *H9*, respectively. The backbone polymer, poly(norbornene diethylester) (Fig. 1, top) was also studied for comparison and two dielectrically active processes were found: a low-temperature Arrhenius process with  $\log(\tau_0/s) = -16.5$ ,  $E_\delta =$

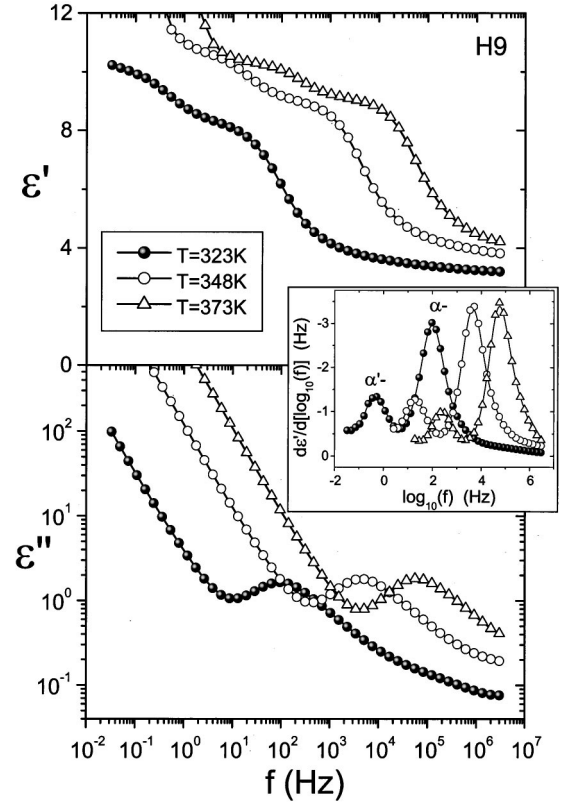


FIG. 4. Dielectric permittivity (top) and loss (bottom) spectra of the SC-PLC *H9* at three temperatures as indicated. In the inset, the derivative of the dielectric permittivity is shown as a function of frequency. The fast and slow processes are indicated as  $\alpha$  and  $\alpha'$ , respectively.

$= 9.95$  kcal/mol, and a relaxation strength of  $T\Delta\varepsilon = 300$ , and a high- $T$  process described with the VFT parameters:  $\log(\tau_0/s) = -11.0$ ,  $B = 797$  K,  $T_0 = 233.5$  K, and with a relaxation strength of  $T\Delta\varepsilon = 400$ .

The low- $T$   $\delta$  relaxation in both SC-PLC originates from the backbone since it has similar activation parameters with the low- $T$  relaxation in poly(norbornene diethylester). Moreover, the dielectric strengths ( $T\Delta\varepsilon$ ) of 100 and 50 in the *H3* and *H9* polymers, respectively, can be understood in terms of a dilution of the ester dipoles by the side chains. The weak ( $T\Delta\varepsilon = 2-3$ )  $\gamma$  process, on the other hand, does not relate to the backbone since it is only observed in the *H3* and *H9* SC-PLC. This process may originate from a very local motion of the side chains without involving the motion of the mesogenic group. By increasing  $T$ , another Arrhenius process (called the  $\beta$  process, Fig. 5) is detected in the *H3* polymer. Traces of the same process could also be observed in the *H9* polymer, however, with much less intensity, which made the decomposition impossible. The signature of this process is the increasing dielectric strength with increasing  $T$  ( $T\Delta\varepsilon$  from 40 to 200), suggesting the unfreezing of the side-chain dipoles. At even higher temperatures, the *H3* polymer exhibits the segmental ( $\alpha$ ) relaxation which is unaffected by the nematic-to-isotropic transition. In contrast, the smectic-*A* forming SC-PLC *H9* has two VFT relaxations ( $\alpha$  and  $\alpha'$ ) that “freeze” practically at the same temperature  $T_0$ . The

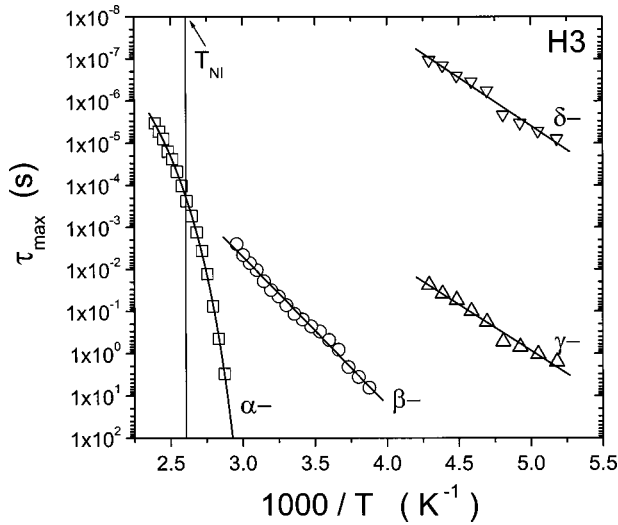


FIG. 5. Temperature dependence of the relaxation times for the different processes in the SC-PLC *H3* plotted in the usual Arrhenius representation. The different processes are indicated by the Greek letters  $\delta, \gamma, \beta, \alpha$  by increasing temperature. The vertical line signifies the nematic-to-isotropic transition. Notice that the  $\alpha$  process is continuous throughout the transition.

shift in the “ideal” glass transition temperatures of *H3* and *H9* polymers reflects the reduction of the glass transition temperatures as measured by DSC (Table I) resulting from the internal plasticization due to the longer side chain. Furthermore, the intensity of the  $\alpha$  process in the *H3* and *H9* polymers is  $T\Delta\varepsilon = 2500$  and  $2000$ , respectively; being higher than the backbone is likely to reflect the cooperative dynamics of the whole system, backbone and side chains but with a dominant contribution from the mesogen.

On the other hand, the  $\alpha'$  process in the *H9* polymer

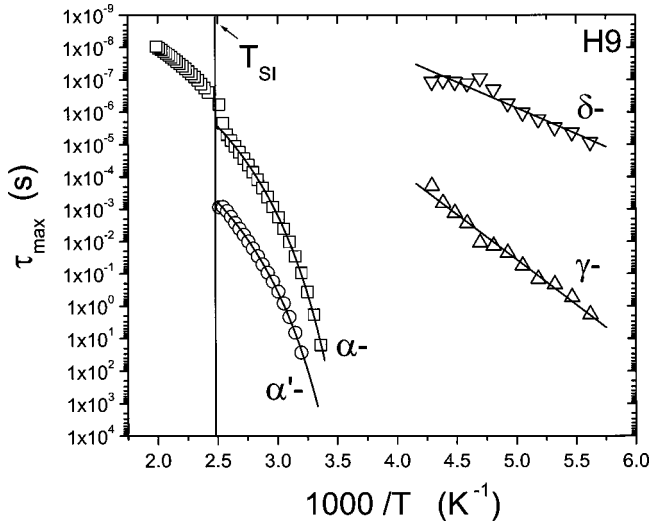


FIG. 6. Temperature dependence of the relaxation times for the different processes in the SC-PLC *H9* plotted in the usual Arrhenius representation at 1 bar. The different processes are indicated by the Greek letters  $\delta, \gamma, \alpha, \alpha'$  by increasing temperature. The vertical line signifies the smectic-to-isotropic transition (at 1 bar). Notice the speed-up of the  $\alpha$  process at the transition.

TABLE II. Activation parameters for the relaxation processes in the *H3* polymer.

<i>H3</i> polymer	$\alpha$	$\beta$	$\gamma$	$\delta$
$\log(\tau_0/s)$	-9.9	-12.9	10.9	-16.8
$E$ (kcal/mol)		16.1	10.9	10.4
$B$ (K)	$550 \pm 30$			
$T_0$ (K)	$295 \pm 1.5$			

reflects a cooperative relaxation that is influenced by the local smectic order. This relaxation is coupled to the  $\alpha$  process since both processes have similar VFT parameters, suggesting that they freeze at the same temperature. In many cases the slow ( $\alpha'$ ) relaxation has been attributed to the reorientation of the longitudinal component of the dipole moment in the side-chain mesogen ( $\mu_l = 4.2$  D), originating from the cyanobiphenyl end group (-CN), around the backbone. The faster  $\alpha$  process was also attributed to the transverse dipole moment originating from the oxy-group ( $\mu_t \approx 2$  Debye) rotating about the mesogens' long axis. Such an assignment, however, would suggest that the slower process would be the more intense, which does not agree with our finding that the intensity of the slow process is only a fraction of the intensity of the  $\alpha$  process (Fig. 4). Furthermore, the double bonds on the norbonene backbone (Fig. 1) do not allow for a complete reorientation of the mesogen around the backbone. A more plausible assignment of the  $\alpha'$  process is of a local reorientation of the side chains between different smectic layers. Moreover, the absence of the  $\alpha'$  process in the *H3* polymer may reflect the lower order within the weak nematic phase.

It is interesting to note that (i) the  $\alpha$  process accelerates on passing into the isotropic regime and (ii) that the  $\alpha'$  process persists despite being very weak within the isotropic phase (dashed line in Fig. 6). The acceleration of the  $\alpha$  process at the smectic-to-isotropic transition reflects the change in local friction due to the randomization of the mesogen and backbone motions in the isotropic phase. On the other hand, the existence of a weak  $\alpha'$  process (see Fig. 10) in the isotropic phase, which was not been reported before, is suggestive of some kind of local order. The weak  $\alpha'$  process observed in the dynamics may reflect pretransitional effects originating from the enhanced static short-range order at  $T > T_c$ . Such pretransitional effects have been reported for polymers composed of a nematogenic backbone and long spacers to occur at  $T - T_c \approx 10$  K [29]. The origin of the local order is the stiffening of the backbone prior to the transition

TABLE III. Activation parameters for the relaxation processes in *H9* polymer.

<i>H9</i> polymer	$\alpha'$	$\alpha$	$\gamma$	$\delta$
$\log(\tau_0/s)$	-7.2	-9.6	-15.4	-14.1
$E$ (kcal/mol)			12.8	7.3
$B$ (K)	$659 \pm 30$	$658 \pm 20$		
$T_0$ (K)	$236.5 \pm 2$	$236.5 \pm 1$		

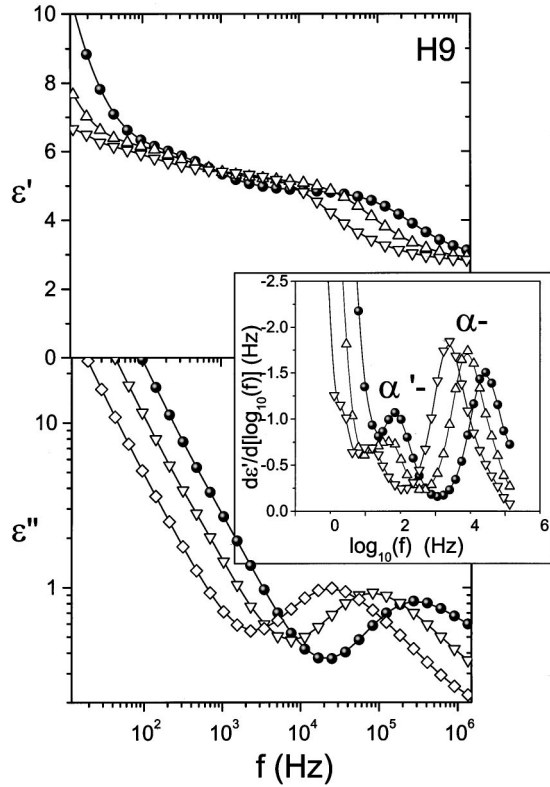


FIG. 7. Dielectric permittivity (top) and loss (bottom) spectra of the SC-PLC *H9* at  $T=393$  K shown for three pressures: (●)  $P=1$  bar, (△)  $P=0.5$  kbar, (▽)  $P=1$  kbar. In the inset the derivative of the dielectric permittivity is shown and the two processes are indicated as  $\alpha$  and  $\alpha'$ .

which is described by a persistence length  $l_p$  increasing with the square of the nematic correlation length  $\xi$ , as  $l_p \sim \xi^2/a$ , where  $a$  is the monomer size. Hence,  $\xi/a > 1$  results in  $l_p > \xi$  and in this regime chains appear as rigid already above  $T_c$ . The increasing smectic correlation length prior to the transition may also influence the persistence length of the backbone and result in some local order above the transition temperature.

To gain a further insight into the dynamics of the  $\alpha$  and  $\alpha'$  processes in the *H9* polymer and of the  $\alpha$  and  $\beta$  processes in the *H3* polymer, we have studied the response of the different processes under external pressure. The result of applying pressure on the dielectric spectra of the *H9* polymer is shown in Fig. 7. By increasing pressure, the two relaxation processes (which are better resolved by the derivative method) are shifted to longer times. The corresponding pressure dependence of the relaxation times of the two processes is depicted in Fig. 8 for several temperatures below but also above the  $T_{SI}$  (as obtained at 1 bar). Both processes display a linear dependence on pressure, within the investigated pressure range, with the  $\alpha$  process showing a stronger dependence as compared to the slow  $\alpha'$  process. The fact that the two processes approach each other both by decreasing  $T$  and increasing  $P$  suggest a common relaxation mechanism at  $T_g$  and  $P_g$ . The linear dependencies found in Fig. 8 can result through completely different approaches [30]. The first approach is based on transition state theory and the lin-

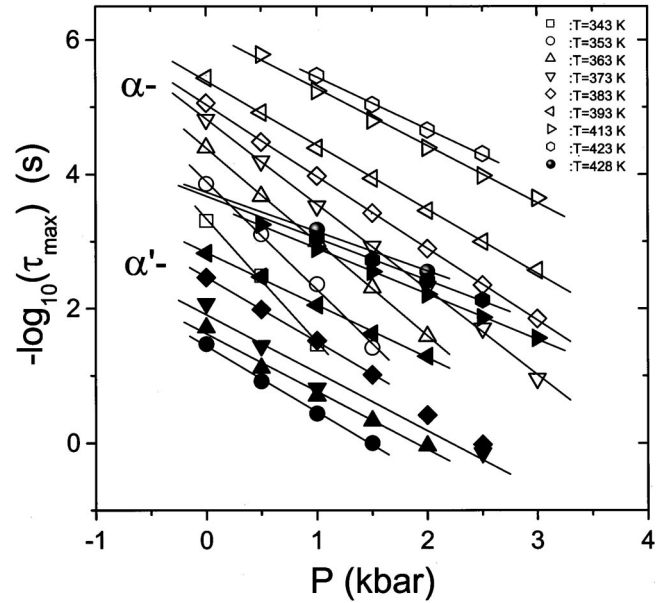


FIG. 8. Pressure dependence of the relaxation times corresponding to the maximum loss for the  $\alpha$  (open symbols) and  $\alpha'$  (filled symbols) processes in the *H9* polymer for different temperatures as indicated. The lines are the result from linear fits (see text).

ear dependence can be used to define an activation volume  $\Delta V$

$$\Delta V = RT \left( \frac{\partial \ln \tau}{\partial P} \right)_T, \quad (4)$$

where  $\Delta V$  is the difference in the molar volumes of activated and nonactivated species. A similar  $\tau(P)$  dependence can result from a second approach which is based on the free volume theory. In this case, a model of variable free volume compressibility results in the definition of a characteristic volume  $\Delta V$  which is also described by Eq. (4). We refer to this volume also as “activated volume” because of the similarity to Eq. (4).

The activation volumes obtained from the linear fits of Fig. 8 to the  $\alpha$  and  $\alpha'$  processes are shown in Fig. 9 as a function of temperature. Both decrease with increasing  $T$ ; however, the volume associated with the  $\alpha$  process displays a much stronger dependence. The two dependencies could be parametrized as  $\Delta V_\alpha = 1550 - 6.9T + 0.008T^2$  and  $\Delta V_{\alpha'} = 130 - 0.184T$  ( $T$  in K). The former dependence is reminiscent of the strong  $\Delta V(T)$  found in the segmental modes of polyisoprenes of different molecular weights and the strong increase could imply a correlation with the cooperative volume.

Apart from slowing down the smectic-*A* phase dynamics, pressure can be used to test some basic thermodynamic principles. For a first-order transition, the Clausius-Clapeyron equation predicts that pressure should increase the transition temperature provided that the transition is accompanied by a positive volume change, as

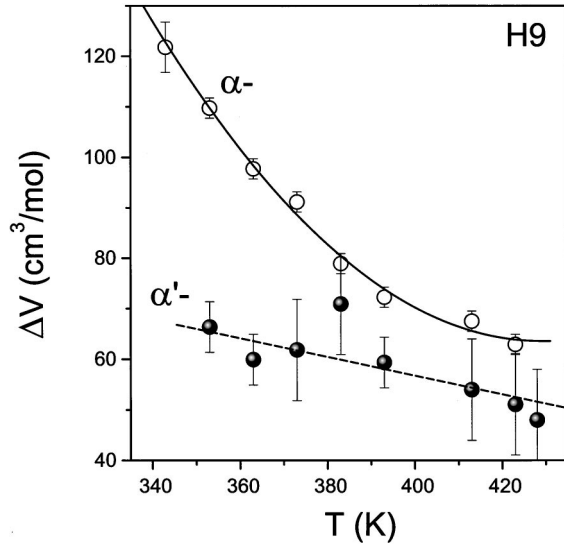


FIG. 9. Apparent activation volumes for the  $\alpha$  (open symbols) and  $\alpha'$  (filled symbols) processes in the  $H9$  polymer as a function of temperature. The lines are to guide the eye.

$$\frac{dP}{dT} = \frac{\Delta H}{T\Delta V}. \quad (5)$$

In the above equation,  $\Delta H$  is the latent heat associated with the smectic-to-isotropic transition and  $\Delta V$  is the change in specific volume at the transition. We have followed the effect of pressure on the  $T_{SI}$  by studying the spectral changes imposed by pressure on the isotropic phase dynamics of the  $H9$  polymer. As mentioned earlier, the isotropic phase spectra, at atmospheric pressure, are influenced by the strong  $\alpha$  process and by a very weak process whose dynamics lie in the ex-

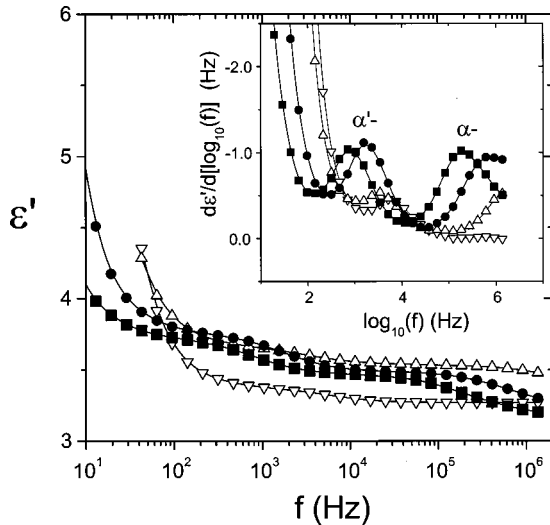


FIG. 10. Dielectric permittivity spectra of the  $H9$  polymer at 433 K (corresponding to the isotropic phase at atmospheric pressure) plotted for different pressures: ( $\nabla$ )  $P=1$  bar, ( $\Delta$ )  $P=0.5$  kbar, ( $\bullet$ )  $P=1$  kbar, ( $\blacksquare$ )  $P=1.5$  kbar. In the inset, the derivative of the dielectric permittivity is shown. The strong dual relaxation is used to define a critical pressure needed to induce the isotropic-to-smectic transformation.

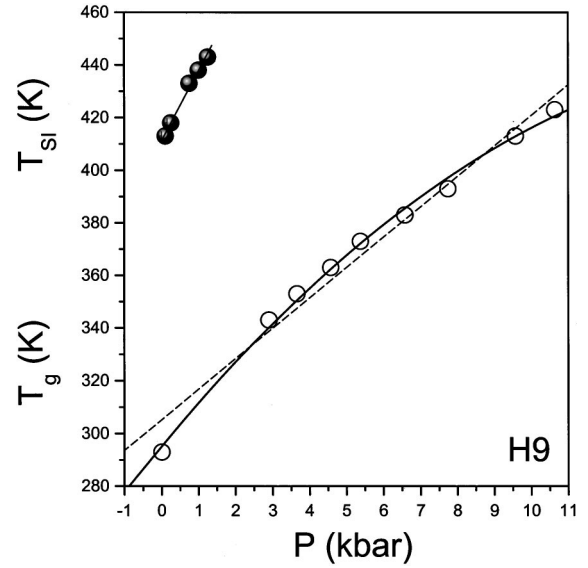


FIG. 11. Pressure dependence of the glass transition temperature  $T_g$  (open symbols) and of the isotropic-to-smectic transition temperature (filled symbols). The  $T_g$  was operationally defined as a temperature corresponding to a relaxation time of 100 s. The dashed and solid lines represent linear and nonlinear fits to the  $T_g(P)$  data points (see text). The line  $T_{SI}(P)$  represents a linear fit to the data points.

trapolation of the  $\alpha'$  process from the smectic mesophase. By applying pressure, both processes become slower but, in addition, there is a critical pressure  $P_c$ , above which the slow  $\alpha'$  process intensifies reflecting an induced smectic-to-isotropic transition by pressure. This situation is shown in Fig. 10 where some representative  $H9$  spectra are shown at 433 K, that is, well within the isotropic phase at 1 bar. Increasing the applied pressure above some critical value (which is  $T$  dependent) results in the induction of the isotropic-to-smectic transition.

The  $T_{SI}(P)$  and  $T_g(P)$  dependencies in the  $H9$  polymer (here the  $T_g$  is operationally defined as the temperature corresponding to a relaxation time for the  $\alpha$  process of 100 s) are compared in Fig. 11. Pressure increases both characteristic temperatures, but the effect is more pronounced in the former due to the first-order nature of the transition. From the linear  $T_{SI}(P)$  dependence we obtain

$$\frac{dT_{SI}}{dP} = 26.4 \frac{\text{K}}{\text{kbar}}, \quad (6)$$

a dependence much stronger than the  $dT_g/dP = 11.6 \text{ K/kbar}$  found if a linear regression is used to describe the  $T_g(P)$  dependence. However, a nonlinear dependence can better approximate the latter, i.e.,  $T_g(P) = 295 + 16.9P - 0.48P^2$  ( $T$  in K,  $P$  in kbar). The stronger  $T_{SI}(P)$  than  $T_g(P)$  dependence results in a greater  $T_{SI}(P) - T_g(P)$  at higher pressures. This leads to an apparently paradoxical situation where the pressurized smectic liquid just below the isotropic transition is more mobile than the smectic liquid obtained at atmospheric pressure. We can now employ the Clausius-Clapeyron equation to estimate the change of spe-

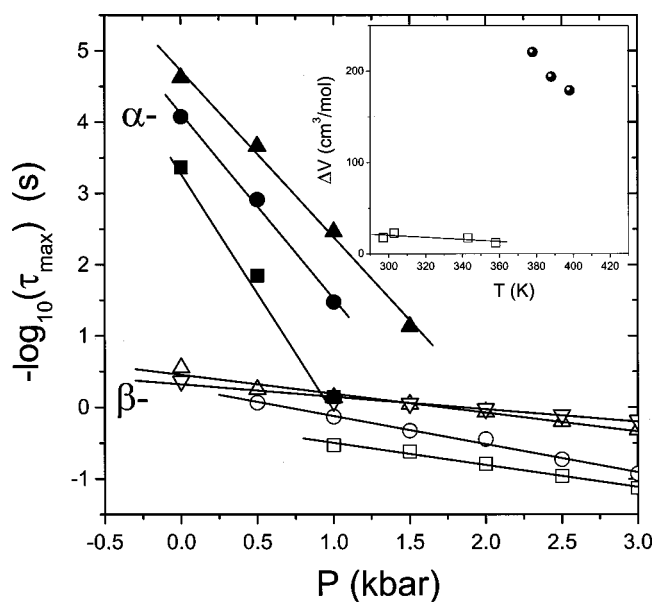


FIG. 12. Pressure dependence of the relaxation times corresponding to the maximum loss for the SC-PLC H3. Two processes are shown: the  $\alpha$  (filled symbols) and the  $\beta$  process (open symbols). The different temperatures are ( $\blacktriangle$ ) 398 K, ( $\bullet$ )  $T=388$  K, ( $\blacksquare$ )  $T=378$  K, ( $\nabla$ )  $T=358$  K, ( $\triangle$ )  $T=343$  K, ( $\circ$ )  $T=303$  K, ( $\square$ )  $T=297$  K. In the inset, the apparent activation volume is plotted for the two processes as a function of temperature.

cific volume at the transition assuming that pressure does not affect the heat content. Under this premise, at  $T=408$  K, we obtain a change in the specific volume of  $0.0032$   $\text{cm}^3/\text{g}$ . The latter is in good agreement with the measured change in specific volume at the smectic-to-isotropic transition of other side-chain liquid-crystalline polymers [31].

We have also examined the effect of pressure on the  $\alpha$  and  $\beta$  relaxations in the H3 polymer. Based on their distinctly different temperature dependence, the expectation is that the two processes will display also different pressure dependencies due to the different volume requirements. The result of the analysis of the relaxation times at maximum loss is shown in Fig. 12 as a function of pressure. According to the expectation, pressure is found to shift the  $\alpha$  process much

more than the glassy  $\beta$  process and thus to lead to a better separation of the two processes. Clearly, the  $\beta$  process is less volume demanding as anticipated by its weak Arrhenius-like  $T$  dependence. The characteristic volumes, shown in the inset, reveal a low and nearly independent  $\Delta V$  for the  $\beta$  process as compared to the much higher and  $T$  dependent  $\Delta V$  associated with the segmental process. The latter results in a  $dT_g/dP$  of  $18.7$  K/kbar, which is somewhat higher than in the H9 polymer.

#### IV. CONCLUSIONS

The dielectric investigation of the dynamics in two side-chain liquid-crystalline derivatives of polynorbornene, forming smectic-A and nematic mesophases, revealed multiple dynamic processes. The main result of the  $T$ - and  $P$ -dependent investigation can be summarized as follows.

(i) The segmental ( $\alpha$ ) process in the two SC-PLC reflects the dynamic glass transition which is shifted to lower temperatures in the polymer with the longer spacer due to the internal plasticization.

(ii) The nematic-to-isotropic transition has no measurable effect on the dynamics at the length scale of the  $\alpha$  process; however, the smectic-to-isotropic transition is accompanied by a speed-up reflecting the randomization of dipoles.

(iii) The  $\alpha$  and the slower  $\alpha'$  process found in the smectic mesophase merge by decreasing temperature and by increasing pressure, suggesting a common relaxation mechanism.

(iv) Pressure increases the glass transition temperatures of the H3 and H9 polymers as  $dT_g/dP=18.7$  and  $16.9$  K/kbar, respectively, but has a weak effect on the  $\beta$  process of the H3 polymer.

(v) Pressure exerts a strong influence on inducing the first-order isotropic-to-smectic transition as  $dT_{SI}/dP=26.4$  K/kbar, and this value is in agreement with the expected volume change at the transition.

#### ACKNOWLEDGMENTS

We thank Professor J. Dorgan for his comments on the manuscript. M. M. thanks the Polish Science Foundation (FNP'2000) for financial support.

- [1] H. Finkelmann and G. Rehage, *Adv. Polym. Sci.* **60**, 99 (1984).
- [2] V. P. Shibaev and N. A. Plate, *Adv. Polym. Sci.* **60**, 173 (1984).
- [3] H. Finkelmann, H. Ringsdorf, W. Siol, and J. H. Wendorff, *ACS Symp. Ser.* **74**, 22 (1978).
- [4] W. Haase, H. Pranoto, and F. J. Bormuth, *Ber. Bunsenges. Phys. Chem.* **89**, 1229 (1985).
- [5] F. J. Bormuth, A. M. Biradar, U. Quotschalla, and W. Haase, *Liq. Cryst.* **5**, 1549 (1989).
- [6] S. Götz, W. Stille, G. Strobl, and H. Scheuermann, *Ber. Bunsenges. Phys. Chem.* **97**, 1315 (1993).
- [7] Z. Z. Zhong, D. E. Schuele, and W. L. Gordon, *Liq. Cryst.* **17**, 199 (1994).
- [8] S. U. Vallerien, F. Kremer, and C. Boeffel, *Liq. Cryst.* **4**, 79 (1989).
- [9] Ch. Cramer, Th. Cramer, F. Kremer, and R. Stannarius, *J. Chem. Phys.* **106**, 3730 (1997).
- [10] S. A. Rozanski, F. Kremer, H. Groothues, and R. Stannarius, *Mol. Cryst. Liq. Cryst. Sci. Technol., Sect. A* **303**, 319 (1997).
- [11] A. Schönals, D. Wolff, and J. Springer, *Macromolecules* **28**, 6254 (1995).
- [12] A. Schönals, D. Wolff, and J. Springer, *Macromolecules* **31**, 9019 (1998).
- [13] J. Mijovic and J.-W. Sy, *Macromolecules* **33**, 9620 (2000).
- [14] G. S. Attard, *Mol. Phys.* **58**, 1087 (1986).
- [15] G. S. Attard, K. Arakia, and G. Williams, *Br. Polym. J.* **19**, 119 (1987).
- [16] W. Maier, G. Meier, and A. Saupe, *Faraday Symp. Chem. Soc.* **5**, 119 (1975).

- [17] W. Heinrich and B. Stoll, *Colloid Polym. Sci.* **263**, 895 (1985).
- [18] G. Williams, *Trans. Faraday Soc.* **60**, 1548 (1964); **60**, 1556 (1964).
- [19] H. Sasabe and S. Saito, *J. Polym. Sci., Part A: Polym. Chem.* **6**, 1401 (1968).
- [20] G. Floudas and T. Reisinger, *J. Chem. Phys.* **111**, 5201 (1999).
- [21] G. Floudas, C. Gravalides, T. Reisinger, and G. Wegner, *J. Chem. Phys.* **111**, 9847 (1999).
- [22] G. Floudas, G. Fytas, T. Reisinger, and G. Wegner, *J. Chem. Phys.* **111**, 9129 (1999).
- [23] M. Mierzwa, G. Floudas, P. Stepanek, and G. Wegner, *Phys. Rev. B* **62**, 14 012 (2000).
- [24] M. Mierzwa and G. Floudas, *IEEE Trans. Dielectr. Electr.* **8**, 359 (2001).
- [25] M. Ungerank, B. Winkler, E. Eder, and F. Stelzer, *Macromol. Chem. Phys.* **196**, 3623 (1995).
- [26] A. Wewerka, G. Floudas, T. Pakula, K. Viertler, and F. Stelzer (unpublished).
- [27] M. Wübbenhorst, E. Van Koten, J. Jansen, M. Mijs, and J. van Turnhout, *Macromol. Rapid Commun.* **18**, 139 (1997).
- [28] S. Havriliak and S. Negami, *Polymer* **8**, 161 (1967).
- [29] P.-G. de Gennes, *Mol. Cryst. Liq. Cryst.* **102**, 95 (1984).
- [30] G. Floudas, in *Broadband Dielectric Spectroscopy*, edited by F. Kremer and A. Schönhalz (Springer, Berlin, 2001), Chap. 8.
- [31] J. Frenzel and G. Rehage, *Makromol. Chem.* **184**, 1685 (1983).